Theoretical and experimental analysis of conductivity, ion diffusion and molecular transport during cell electroporation — Relation between short-lived and long-lived pores

Mojca Pavlin *, Damijan Miklavčič

University of Ljubljana, Faculty of Electrical Engineering, Tržaška 25, SI-1000 Ljubljana, Slovenia

ARTICLE INFO

ABSTRACT

Electroporation is usually described as a formation of transient pores in the cell membrane in the presence of a strong electric field, which enables transport of molecules and ions across the cell membrane. Several experimental studies of electroporation showed a complex dependence of the transport on pulse parameters. In only few studies, however, the actual transport across the membrane was quantified. Current theoretical studies can describe pore formation in artificial lipid membranes but still cannot explain mechanisms of formation and properties of long-lived pores which are formed during cell electroporation. The focus of our study is to connect theoretical description of pore formation during the electric pulses with experimental observation of increased transport after the pulses. By analyzing transient increase in conductivity during the pulses in parallel with ion efflux after the pulses the relation between short-lived and long-lived pores was investigated. We present a simple model that incorporates an increase in the fraction of long-lived pores with higher electric field due to larger area of the cell membrane exposed to above-critical voltage and due to higher energy which is available for pore formation. We also show that each consecutive pulse increases the probability for the formation of long–lived pores.

© 2008 Elsevier B.V. All rights reserved.

1. Introduction

The cell membrane has low permeability for most molecules and ions due to the hydrophobic nature of the lipid bilayer. Transport through the membrane occurs only for certain molecules and ions through membrane channels by means of diffusion or by active transport.

However, for different biomedical applications it is useful to increase permeability of the membrane to introduce certain drugs or molecules into the cell. A few decades ago it was shown that strong electric fields can cause structural changes in the cell membrane, which result in increased permeability for ions and larger molecules [1]. This process was named electroporation since it is believed that pores are formed in the cell membrane during the presence of the electric field which dramatically increases transport of water soluble ions and molecules across the membrane [2,3]. Sometimes the term electropermeabilization is used instead to stress that increased permeability is observed. Electroporation is currently an established method for delivery of molecules into cells in vitro and in vivo, as well as an integral part of electrochemotherapy of tumors [4–6] and gene electrotransfer [7–9]. Several recent studies [9–11] in vivo suggested that gene electrotransfer could become important method for DNA transfer

in gene therapy of various illnesses as an alternative method to the viral transfection, while electrochemotherapy is starting to become used in clinics as a possible therapy for cutaneous and subcutaneous tumors [9,12]. However, even though electroporation is already widely used in vitro experiments and successfully used for clinical applications, up to now there is no complete description on the molecular level.

In general, the key parameter for successful cell permeabilization is the induced transmembrane voltage [2,3,13,14] which is generated by an external electric field due to the difference in the electric properties of the cell membrane, external medium and cytoplasm known as the Maxwell–Wagner polarization [3]. The induced transmembrane voltage on a cell membrane can be derived from the solution of a Laplace equation. For physiological values of parameters when the cell membrane is almost non–conductive [2,3] we obtain for the transmembrane voltage of a spherical cell:

$$U_{\mathrm{m}} = \frac{3}{2} E_0 R \cos \theta, \tag{1}$$

where E_0 is the applied electric field, R radius of the cell and θ the angle between the field direction and radius vector to the given point on the membrane. The cell membrane becomes permeable for transmembrane voltages above a certain threshold, which was estimated to be between 200 mV and 1 V [2,3,13–15]. After pulse application the process of resealing takes several minutes allowing for transport of molecules and ions across the cell membrane. However,

* Corresponding author. Tel.: +386 1 4768 768; fax: +386 1 4264 658.
E-mail addresses: mojca.pavlin@fe.uni-lj.si (M. Pavlin),
damijan.miklavcic@fe.uni-lj.si (D. Miklavčič).

electroporation is reversible only for a given range of parameters of electric pulses. When an electric field is further increased or for longer pulses or for larger number of pulses the changes in the cell structure become irreversible finally leading to its death.

Electroporation was experimentally studied on all levels of biological complexity from planar lipid bilayer membranes (usually referred as dielectric breakdown), single cells, cells in suspensions, to in vivo experiments [2,3,13,14]. Although there is a lot of indirect experimental evidence of the increased membrane permeability and studies of the effects of different parameters on the efficacy of electroporation, these observations alone do not explain the underlying physical–chemical mechanisms, which cause structural changes of the membrane and finally lead to its increased permeability long after the electric pulses are switched off [14,16]. Also none of the existing experimental methods enable direct visualization of pores — i.e. permeable structures in the cell membrane. Recently, molecular-dynamics studies showed formation of aqueous pores in the lipid bilayer in a very strong nanoseconds long electric field pulses [17], which is in agreement with experimental observation of electroporation and bioelectric effects observed with nanoseconds pulses [18]. However, current molecular molecular-dynamics simulations are limited to short nanosecond time–scale, while "classical" electroporation occurs in microsecond time–scale.

In parallel with experimental data several theoretical models were developed from which the model of aqueous pore formation offers the most accurate agreement with observations [14,19–22]. Still, this theoretical model was developed and validated on experiments on bilayer membranes or by measuring transient conductivity changes — therefore in both cases by studying only transient short-lived permeable structures with life-time of milliseconds [19,21]. In contrast to this, all experimental data on cell electroporation agree, that life-time of pores, which enable molecular diffusion, range from minutes to hours depending on pulse parameters and temperature, which is crucial for biomedical and biotechnological applications. It is therefore clear that complete description of cell electroporation is still lacking connection between experimental data and the theoretical framework [14,16].

Only in few studies, which studied conductivity changes and ion diffusion during cell electroporation authors directly observed and analyzed the actual transport across the membrane [23–29]. For this reason we made and extensive study of the effect of cell electroporation on ion permeability during the electric pulses and ion diffusion after electric pulses on dense cell suspension of B16F1 (mouse melanoma) cells. The main objective of the present study is to understand the relation between short-lived pores and long-lived pores in cell electroporation as well as to interpret the experimental data in the framework of known theoretical models of increased membrane conductivity, effective conductivity and ion diffusion across the permeabilized membrane.

We measured conductivity of a cell suspension during application of electrical pulses as well as after pulse application using low-voltage test pulses. In parallel, experiments of molecular uptake were performed. From measured conductivity, ion diffusion and molecular transport using theoretical models we quantify the fraction of short-lived and long-lived pores. We also determine time constant of the short-lived pores. We further analyze which parameters affect stabilization of the long-lived pores and discuss the relation between the short-lived transient pores and the long-lived pores. The other objective of this study is to asses if conductivity measurement could be used as a method for an on-line detection of cell electroporation in vitro and/or in vivo as previously suggested [26,29,30].

2. Materials and methods

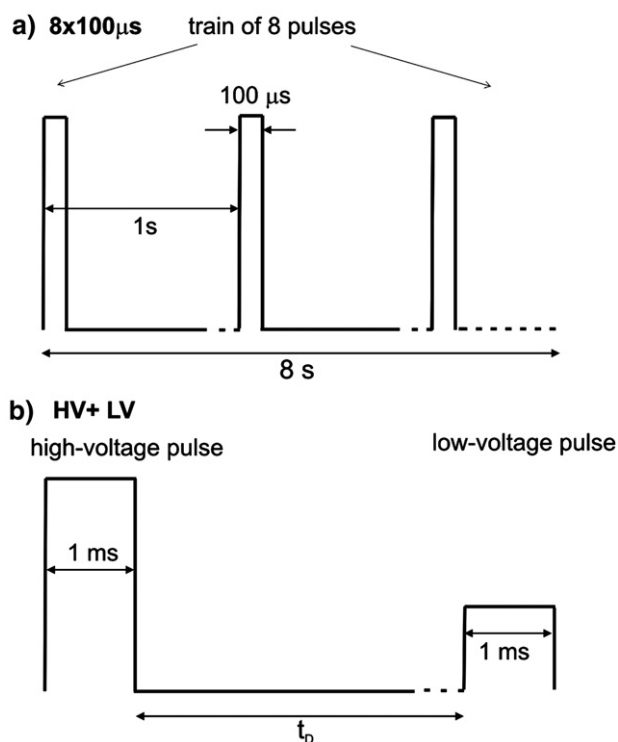### 2.1. Electroporation and current–voltage measurements

The experimental setup consisted of a generator that delivered square pulses, an oscilloscope and a current probe. Two high-voltage generators were used; for protocol where 8×100 µs pulses were used a prototype developed at the University of Ljubljana, Faculty of Electrical Engineering, was used and for the second protocol Cliniporator™ device (IGEA s.r.l., Carpi, Modena, Italy) was used, which allowed us to deliver combination of one high-voltage and one low-voltage pulse with a given delay in between.

During the pulses the electric current was measured with a current probe (LeCroy AP015, New York, USA) and the applied voltage with the high-voltage probe (Tektronix P5100, Beaverton, USA). Current and voltage were measured and stored on the oscilloscope (LeCroy 9310 C Dual 400 MHz, New York, USA). In the first type of experiments we used a protocol using train of eight square pulses of 100 µs duration with 1 Hz repetition frequency — the 8×100 µs protocol (in one experiment the repetition frequency was changed). Parallel aluminum plate electrodes (Eppendorf cuvettes) with $d = 2$ mm distances between the electrodes were used. Pulse amplitudes were varied to produce applied electric field $E_0 = U/d$ between 0.4 kV/cm and 1.8 kV/cm. In the second type of experiments first one 1 ms high-voltage (HV) pulse was delivered, and after a given delay of (0.1 ms–4200 ms) one 1 ms low-voltage (LV) test pulse was delivered (HV+LV protocol). The applied voltages were $U_{HV} = 200$ V and $U_{LV} = 40$ V, which gave applied electric field $E_{0\ HV} = 1$ kV/cm and $E_{0\ LV} = 0.2$ kV/cm. For every set of parameters a reference measurement on medium with no cells was also performed.

2.2. Cells

In all experiments cell suspension of mouse melanoma cells (B16F1) were used. Cells were grown in Eagle's minimum essential medium supplemented with 10% fetal bovine serum (Sigma-Aldrich Chemie GmbH, Deisenhofen, Germany) at 37 °C in a humidified 5% CO_2 atmosphere in the incubator (WTB Binder, Labortechnik GmbH, Germany). The cell suspension was prepared from confluent cultures
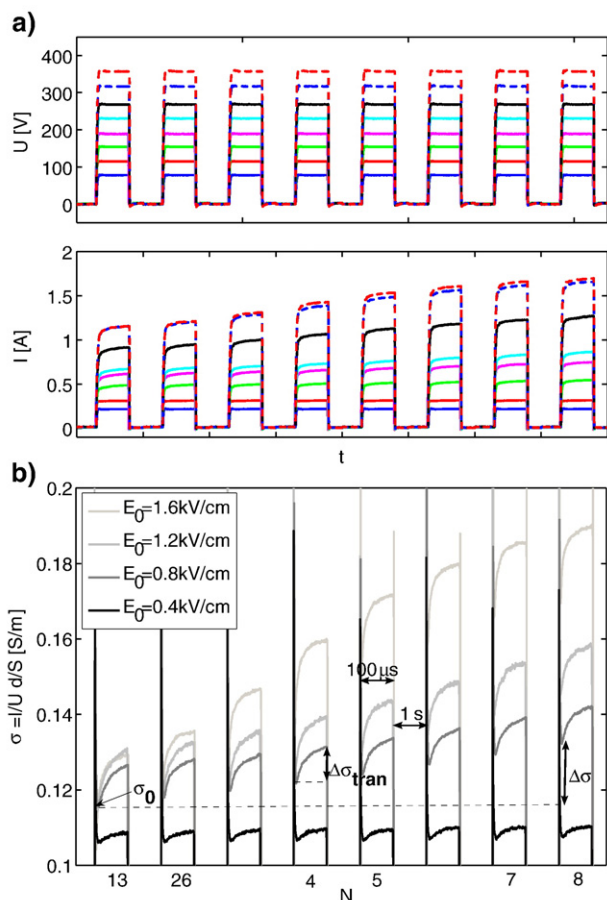

Fig. 1. Schematic representation of the two pulsing protocols which were used: a) a protocol with a train of eight pulses with applied electric field between 0.4 kV/cm and 1.8 kV/cm (8×100 µs) and b) combination of one high-voltage and one low-voltage pulse (HV+LV protocol), where t_D is the time delay between HV and LV pulse, $E_{0\ HV} = 1$ kV/cm and $E_{0\ LV} = 0.2$ kV/cm.
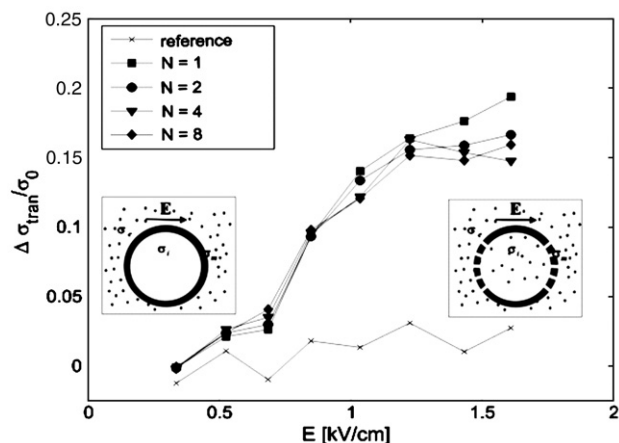
with 0.05% trypsin solution containing 0.02% EDTA (Sigma-Aldrich Chemie GmbH, Deisenhofen, Germany). From the obtained cell suspension trypsin and growth medium were removed by centrifugation at 1000 rpm at 4 °C (Sigma, Germany) and the resulting pellet was resuspended in medium and again centrifuged. A low-conductive medium was used for electroporation that contained phosphate buffer (Na_2HPO_4/NaH_2PO_4) with 250 mM sucrose (PB) σ_0 (25 °C) = 0.127 S/m. In all the experiments dense cell suspensions having cell volume fractions $F = 0.3$ (1×10^8 cells/ml) were used.

3. Results

A typical electroporation experiment consisted of application of electric pulses during which both current and voltage were measured. A low-conductive medium without potassium ions was used to obtain leakage of potassium ions from the cell interior across the permeabilized cell membrane. Two different sets of measurements (see Fig. 1) were made, first with a train of eight pulses 100 µs (usually used in electrochemotherapy), and second using combination of one high-voltage and one low-voltage pulse. From measured voltage and current signals we obtained dynamic conductivity of each sample of cell suspension: $\sigma(t) = I(t)/U(t) \, d/S$, where d is the distance between the electrodes, and S the surface of the sample volume at the electrodes. In the first set of experiments (Fig. 1a) we obtained dynamic conductivity of a cell suspension σ during a train of eight 100 µs pulses

Fig. 2. a) Recorded signals of the measured current I and voltage U during a train of eight 100 µs pulses, 1 Hz repetition frequency for different applied electric fields $E_0 = U/d$ for cells in PB, $E_0 = 0.4$ kV/cm–1.8 kV/cm. b) Time dependent conductivity is shown: $\sigma(t) = I(t)/U(t) \, d/S$. The memory segmentation function of the oscilloscope was used in order to obtain high time resolution during the pulses, and only 100 µs after the pulse were recorded.

Fig. 3. Transient conductivity changes during N-th pulse of the train of 8×100 µs pulses are shown. $\Delta\sigma_{tran}$ is normalized to the initial conductivity. Solid line — cells in low-conductive medium, dotted line — reference measurement on medium without cells during the first pulse. The results are shown against the local electric field E, where $E/E_0 = 0.91$.

and applied electric field between 0.4 kV/cm and 1.8 kV/cm, as shown in Fig. 2b.

In Fig. 2b we define the parameters which we analyzed: $\Delta\sigma_{tran}$ — transient conductivity during the electric pulses and changes of the initial level of conductivity $\Delta\sigma$. The transient conductivity changes are defined as the difference between the final and initial conductivity of the N-th pulse: $\Delta\sigma_{tran} = \sigma^N - \sigma_0^N$ and changes of the initial level (compared to first pulse) as: $\Delta\sigma = \sigma_0^N - \sigma_0$. The initial level of measured conductivity at the start of each pulse (σ_0^N) was determined after a delay of approximately three microseconds after the start of a given pulse, so that fast transient effects due to displacement current and electrode effects were not taken into account (small variations of this delay did not affect significantly the data analysis). The results are normalized to σ_0, which is defined as the initial conductivity at the start of the first pulse $\sigma_0 = \sigma_0^1$.

In the following sections we will analyze both measured quantities: the transient conductivity changes from which we will quantify the transient pores, and the changes of the initial values due to ion efflux from which we will analyze and quantify the long-lived pores.

3.1. Conductivity changes during the pulses — analysis of short-lived pores

3.1.1. Transient conductivity changes

In Fig. 3 transient conductivity changes $\Delta\sigma_{tran}/\sigma_0$ during the N-th 100 µs pulse for $E_0 = U/d = [0.4–1.8]$ kV/cm are shown. Results are presented for different local electric fields E since for a high density of cells is the actual local field smaller than the applied field due to the interaction between the cells [31,32]. The ratio E/E_0 was taken from our previous study [32], where the decrease due to the neighboring cells was calculated to be 9% for volume fraction of cells $F = 0.3$.
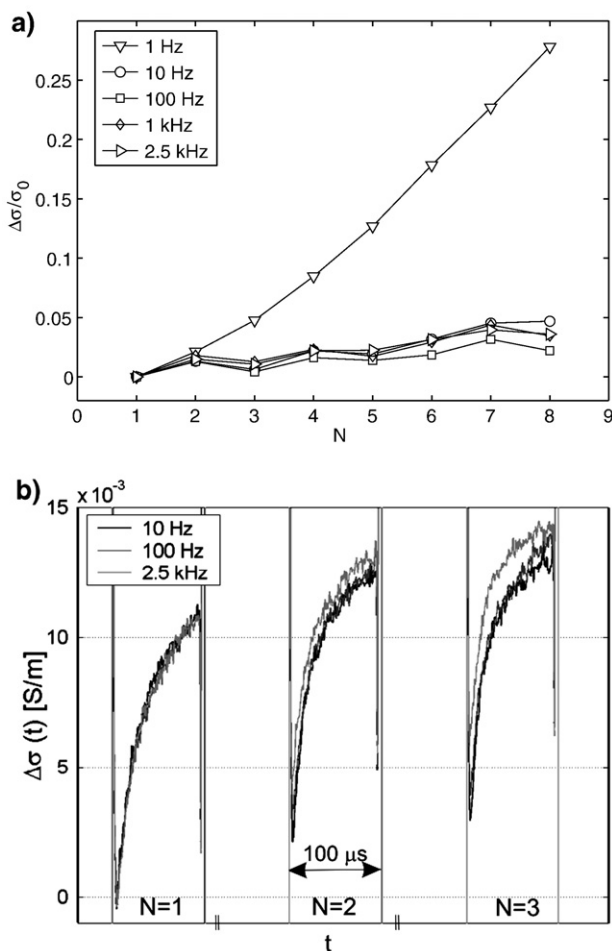
It can be seen that transient conductivity changes during the pulses $\Delta\sigma_{tran}/\sigma_0$ increase considerably above 0.5 kV/cm and reach maximum at 1.2 kV/cm, compared to the reference measurement on pure medium where $\Delta\sigma_{tran}$ are approximately constant (dotted line). The threshold value of 0.5 kV/cm is in agreement with the threshold of molecular uptake which also increases above 0.5 kV/cm, therefore part of the transient conductivity increase can be attributed to formation of short-lived pores in the cell membrane. Surprisingly, the number of pulses does not influence the transient conductivity, which can also be seen directly from the shape of conductivity signals presented in Fig. 2b, where consecutive pulses have very similar shape and increase in transient conductivity.
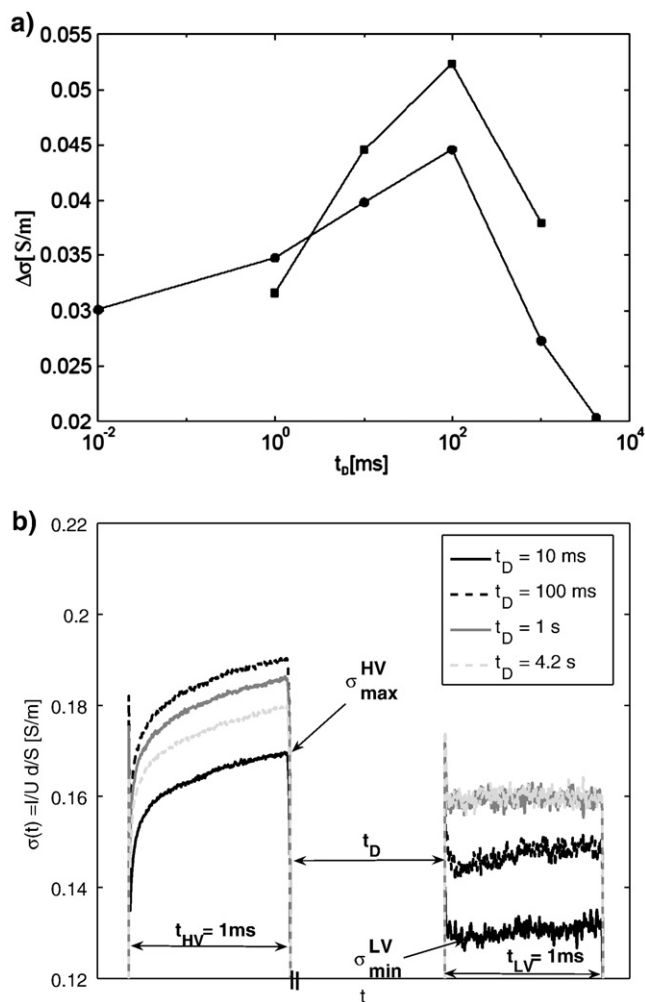
3.1.2. Life-time of short-lived pores

To determine the life-time of transient changes (short-lived pores) we performed a set of experiments where we changed repetition frequency of pulses. So we used a train of 8×100 μs pulses with 1 Hz, 10 Hz, 100 Hz, 1 kHz and 2.5 kHz repetition frequency.

In Fig. 4a the changes of the conductivity between the pulses $- \Delta\sigma/\sigma_0$ (the changes of the initial level) are shown for different repetition frequencies (field dependence on $\Delta\sigma/\sigma_0$ and theoretical analysis will be given in section on ion diffusion). These changes can be explained with ion efflux between the pulses (mostly potassium ions). It can be seen that with an increase in frequency the time interval between consecutive pulses becomes shorter and thus the ion efflux is reduced. For this reason we can neglect the contribution of ion efflux to transient conductivity changes.

In Fig. 4b it is demonstrated that the transient conductivity changes relax almost to the initial level in 10 ms (100 Hz) and after 100 ms the following pulses have almost identical shape as the first pulse. Only for frequencies above 1 kHz (pause between the pulses >1 ms) a significant change in pulse shape occurs and the following pulse starts at higher initial level. These frequencies are presented since the diffusion of ions can be neglected for times shorter than 1 s. For 1 Hz repetition frequency the pulses are almost identical (see Fig. 2b). This indicates that during electric pulses short-lived structural changes are formed which transiently increase ion permeation, but have very short life-time after the pulses, which is around few milliseconds.

Fig. 4. a) Effect of the repetition frequency on the conductivity changes between the pulses (the changes of the initial level) $- \Delta\sigma/\sigma_0$. Pulses 8×100 μs with repetition frequencies 1 Hz, 10 Hz, 100 Hz, 1 kHz and 2.5 kHz were used, $E = 0.84$ kV/cm. b) The time-dependent conductivity signals $\Delta\sigma(t)$ of the first, second and the third pulse with respect to the first pulse are compared for different frequencies.

Fig. 5. a) Conductivity change between high-voltage (HV) and low-voltage (LV) pulse $\Delta\sigma = \sigma_{max}^{HV} - \sigma_{min}^{LV}$ for two experiments (circles and squares), time t_D is the delay between HV and LV pulse. b) Example of the measured signals for one experiment (circles).

In order to further analyze relaxation of transient conductivity changes we performed experiments using combination of a high-voltage (HV) and a low-voltage pulse (LV). In Fig. 5 conductivity changes between the end of the HV pulse and beginning of the test LV pulse: $\Delta\sigma = \sigma_{max}^{HV} - \sigma_{min}^{LV}$ are shown for different delays t_D between the two pulses (see Fig. 5b). Larger conductivity changes between HV and LV pulse represent larger relaxations of the conductivity changes after the pulse. We can see that 10 μs after the pulse the conductivity already drops to 0.03 S/m and after 100 ms it reaches 0.053 S/m. This represents the effect of relaxation after pulse application (resealing of short-lived pores), namely with increasing the delay up to 100 ms the relaxation almost complete (the conductivity drops). Then the effect is reversed due to ion efflux so that few seconds after HV pulse the conductivity of LV pulse is actually increased compared to LV pulse which is delivered immediately after the HV pulse. This is in agreement with our observations of ion efflux in low-conductive media. For delays larger than few seconds osmotic swelling also affect the conductivity, however in our case (delay $t_D < 4.2$ s) it can be neglected [26]. Therefore, we obtained independently that time constant for relaxation of transient conductivity changes and with this the life-time of transient pores is few milliseconds in agreement with results presented in Fig. 4 as well as in agreement with previous studies [33].

3.1.3. Calculation of the fraction of short-lived pores

From the measured transient conductivity changes fraction of the surface area of pores can be determined. The transient change of the

Table 1
Calculation of fraction pores–values of used parameters

n	e/kT	σ_i	D	R
0.15	40 V^{-1}	0.5 S/m	2.5×10^{-5} cm^2/s	8.5×10^{-6} m
E	E_c	w_0	σ_m	d
0.84 kV/cm	0.5 kV/cm	2.5	1.4×10^{-5} S/m	5×10^{-9} m

conductivity $\Delta\sigma_{\mathrm{tran}}$ depends on the average membrane conductivity of the permeabilized area σ_m and critical angle of permeabilized area θ_c and volume fraction of cells. Using Maxwell EMT (effective medium theory) equation [26] we derived a theoretical model [34] which enables calculation of average increased membrane conductivity σ_m of the permeabilized region ($|U_m| > U_c$) from measured transient conductivity changes. A transient increase in conductivity can be explained by the formation of pores in the cell membrane. Therefore we can derive an equation which connects the fraction transient of pores in the cell membrane with membrane conductivity: $\Delta\sigma_{\mathrm{tran}} \Leftrightarrow \sigma_m(E) \Leftrightarrow f_p(E)$.

Detailed derivation is given in our previous studies [26,34]. In general we can assume that the conductance of the permeabilized area of a cell is approximately the sum of the conductance of all pores having radius total surface S_p:

$$G_p = S_{\mathrm{por}} \frac{\sigma_{\mathrm{por}}}{d}, \qquad (2)$$

where we neglect the very small conductance of non-permeabilized cell membrane. This conductance equals the average membrane conductance of the permeabilized area as obtained from our measurement G_{meas}, thus:

$$G_p = G_{\mathrm{meas}} \Rightarrow S_{\mathrm{por}} \frac{\sigma_{\mathrm{por}}}{d} = S_c \frac{\sigma_m}{d}, \qquad (3)$$

where S_c represents the total permeabilized surface of one cell (the area exposed to above-threshold transmembrane voltage — $S_c = S_0 (1 - E_c/E)$ and σ_m the average membrane conductivity of permeabilized area calculated from our measurements according to the theoretical model [26]. From this it follows that the fraction of transient short-lived pores is:

$$f_p = \frac{S_{\mathrm{por}}}{S_0} \approx \frac{(1 - E_c/E)\sigma_m}{\rho \sigma_{0\mathrm{por}}} \qquad (4)$$

where $\sigma_{0\mathrm{por}}$ is average conductivity between inside the cell and extracellular medium and parameter ρ is:

$$\rho = \frac{1}{\left(1 + \frac{n\beta U_m}{w_0 - n\beta U_m}\right) \exp\left(w_0 - n\beta U_m\right) - \frac{n\beta U_m}{w_0 - n\beta U_m}}, \qquad (5)$$

where $\beta = e/kT$ and $w_0 = W_0/kT$, W_0 is the energy of an ion inside center of a pore and n is the relative size of the entrance region of the pore, and was estimated to be approximately 0.15 [21–35]. The values of parameters are presented in Table 1. The parameter ρ takes into account the non-ohmic behavior of the conductivity inside the pore (derivation is given in [21]).

For the average membrane conductivity of the permeabilized area at $E = 0.86$ kV/cm we obtain $\sigma_m = 1.4 \times 10^{-5}$ (detailed calculation is presented in [26]) and inserting values of the parameters (see Table 1) into Eqs. (4) and (5) we obtain the fraction of transient pores for 100 μs long pulse being $f_p \sim 3 \times 10^{-5}$. This is smaller compared to values obtained by other authors [33,36,37], however in the same order of magnitude.

Altogether the conductivity measurements during the pulses enable detection of short-lived permeable structures which are formed during the pulses, but due to fast relaxation (the conductivity drops to initial level in milliseconds after the pulses), these pores do not represent long-lived permeable structures which enable transport of molecules after the pulses.

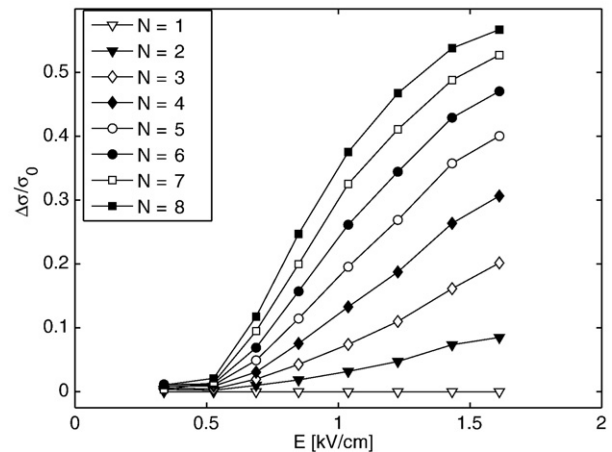### 3.2. Conductivity changes due to ion diffusion — analysis of long-lived pores

3.2.1. Measured conductivity changes due to ion diffusion

In parallel with transient conductivity changes we analyzed the changes of conductivity between the pulses ($\Delta\sigma/\sigma_0$) as defined in Fig. 2b. As already mentioned, these, relatively slow changes in conductivity can be attributed to the ion efflux which occurs between and after the pulse(s). Namely, the ion efflux during the pulses can be neglected due to short duration of the pulses. In Fig. 6 relative changes of the initial level of conductivity at the start of the N-th pulse $\Delta\sigma/\sigma_0 = (\sigma_0^N - \sigma_0)/\sigma_0$ for consecutive pulses are shown for increasing electric field. The results are corrected for the effect of colloid osmotic swelling according to our previous study [26], where we have shown that in few seconds after pulse application swelling of cells significantly reduces the measured conductivity of a cell suspension.

From Fig. 6 it can be seen that similarly as in Fig. 3 the initial level starts to increase above approximately 0.5 kV/cm. This increase can be explained with the efflux of ions (mostly K^+ ions) from the cell interior into the external medium through membrane pores. Namely, inside the cell the initial concentration of potassium is high (140 mM) compared to very low external concentration (few mM) leading to a concentration gradient which drives diffusion of ions across the membrane. Consistently with the transient changes the ion efflux also indicates that the cell membrane is permeabilized above $E = 0.5$ kV/cm. For higher electric fields the efflux of ions increases for higher electric field as well as it increases for larger number of pulses. The relative changes in conductivity due to ion efflux ($\Delta\sigma/\sigma_0$) reached up to 60% increase ($N=8$, $E = 1.6$ kV/cm). Since the observed ion diffusion is observed for several seconds after the pulses, it can be attributed to existence of long-lived pores which enable diffusion of ions and molecules.

3.2.2. Quantification of ion diffusion, flow coefficient and the fraction of long-lived pores

In our analysis we will assume that ion transport during electroporation is governed mostly by diffusion since electromigration during the pulses has effectively no effect on the transmembrane transport (potassium ions on one side are driven into the cell and on the other side out of the cell). An increase in conductivity between the pulses due to ion efflux can be therefore used to determine the permeability of the cell membrane — the flow coefficient and fraction

Fig. 6. The field dependent relative change of conductivity between the pulses (the changes of the initial level) for eight consecutive pulses: $\Delta\sigma/\sigma_0 = (\sigma_0^N - \sigma_0)/\sigma_0$, where σ_0^N is the initial level at the start of the N-th pulse. 8×100 μs pulses were used with repetition frequency 1 Hz, (the pause between the pulses was 1 s).

of long-lived pores which enable molecular transport which is, as already mentioned, crucial for successful use of electroporation in biomedical applications such as electrochemotherapy.

The diffusion of ions is a slow process compared to the duration of the electric pulses thus we can assume that the major contribution to efflux of ions occurs in the absence of the electric field:

$$\frac{dc_e(t)}{dt} = -\frac{DS_{tran}(E,N,t)}{dVF(1-F)}(c_e(t) - Fc_i(t)), \tag{6}$$

where F is volume fraction of the cells, S_{tran} is total area of long-lived pores through which transport occurs and V is the volume of N cells. We can therefore define the fraction of long-lived pores:

$$f_{per} = \frac{S_{tran}}{NS_0} = \frac{S_{por}}{S_0}, S_0 = 4\pi R^2. \tag{7}$$

A more detailed derivation is presented in Appendix A. If we assume that the total surface of pores S_{tran} is approximately constant with time, the solution of the $c_e(t)$ gives an exponential rise to maximum, from which it follows that the conductivity between the pulses also increases as an exponential due to ion efflux. From this it follows that the flow coefficient k_N after the N-th pulse can be determined from the measured conductivity at N-th pulse ($\Delta\sigma_N$) and at $N+1$-th pulse ($\Delta\sigma_{N+1}$) [38]:

$$k_N = \frac{1}{\Delta t_N} \ln\left[1 - \frac{\Delta\sigma_N}{\Delta\sigma_{max}} \middle/ 1 - \frac{\Delta\sigma_{N+1}}{\Delta\sigma_{max}}\right]. \tag{8}$$

The flow coefficient is directly proportional to the fraction of long-lived pores — f_{per}:

$$f_{per} \approx k_N \frac{dR(1-F)}{3D'}, \quad D' = D \exp(-0.43w_0). \tag{9}$$

The relation between measured conductivity changes due to ion efflux and analyzed parameters can be schematically presented as: $\Delta\sigma/\sigma_0 \Leftrightarrow k_N(E,N) \Leftrightarrow f_{per}(E,N)$. Using Eqs. (8) and (9) we obtained the fraction of long-lived pores after a single 100 μs pulse $f_{per} = [0–0.25]\times10^{-5}$ for electric field from 0.5–1.6 kV/cm.

3.2.3. The effect of the electric field on long-lived pore formation and stabilization

It was shown in several studies that the electric field governs the area of the cell membrane, which is exposed to the above-critical transmembrane voltage U_c and has therefore increased permeability according to equation:

$$S_c(E) = S_0(1 - E_c/E). \tag{10}$$

As we have shown in our previous study [38] we can assume (as a first approximation) that pore formation in the area where $U > U_c$ is governed by the free energy of an aqueous pore. Since the permittivity of water differs from membrane permittivity the change of free energy depends in addition to surface and edge energy also on the electrostatic term [14]:

$$\Delta W(r, U_m) = 2\pi\gamma(r)r - \Gamma\pi r^2 - \frac{(\varepsilon_e - \varepsilon_m)\pi r^2}{2d}U_m^2, \tag{11}$$

where Γ is the surface tension ($\sim 1\times10^{-3}$ J. m^{-2}) and γ the edge tension ($\sim 1\times10^{-11}$ J. m^{-1}). If we study the effect of the electric field on the pore formation we can therefore expect that the fraction of long-lived pores and flow coefficient depend on the square of the electric field. Based on this we can assume that the most simplified equation, which describes the field dependent permeability, can be written as [38]:

$$k_N(E) = C_N(1 - E_c/E)E^2 \Rightarrow f_{per}(E) = C_N'(1 - E_c/E)E^2. \tag{12}$$

The constants C_N are in general dependent on the number as well as on the length of pulses, or from a more fundamental perspective, on several parameters which govern evolution of pores size and number. Eq. (12) is a phenomenological equation that takes into account the increase of the area of the cell exposed to the above-critical voltage and the quadratic field dependence in the permeabilized region. For complete theoretical description however, a model should provide formal description on a molecular level as well as incorporate also other parameters such as pulse length and temperature.

As shown in our previous study our phenomenological model is in good agreement with measured flow coefficients and its field dependency. Since the fraction of long-lived pores is approximately proportional to the flow coefficient, we can therefore compare measured and theoretically predicted f_{per}. In Fig. 7 we compare the field dependence of the experimentally determined fraction of pores with the predictions of the model (Eq. (12)). In general are both the flow coefficient k_N and consequently f_{per} functions of several parameters — $f_{per} = f_{per}(E, N, T, t_E, ...)$. It can be seen that f_{per} increases with higher electric field in good agreement with the prediction of the model. The fraction of long-lived pores also increases approximately linearly with number of pulses in agreement with measurements of molecular uptake [26,39–43]. As expected, this is observed only above the threshold electric field. This demonstrates that long-lived pore formation is governed also by the change in the free energy as well as by the number of pulses.

4. Discussion and conclusions

In order to determine the relation between short-lived and long-lived pores during cell electroporation we have to analyze in parallel the quantities which are related to transient changes and the quantities related to long-lived increased permeability of the cell membrane as schematically represented in Fig. 8.

In Table 2 comparison between the measured transient conductivity changes $\Delta\sigma_{tran}/\sigma_0$ during N-th pulse, changes of the initial level due to ion diffusion $\Delta\sigma^N/\sigma_0$ after N pulses, permeability coefficients k_N, the fraction of transient short-lived pores (f_p) and fraction of long-lived pores (f_{per}), and percentage of permeabilized cells at $E = 0.86$ kV/cm are presented.

It can be seen that transient conductivity changes $\Delta\sigma_{tran}/\sigma_0$ and consequently fraction of short-lived pores (f_p) are almost identical for all pulses, whereas fraction of long-lived pores (f_{per}) and
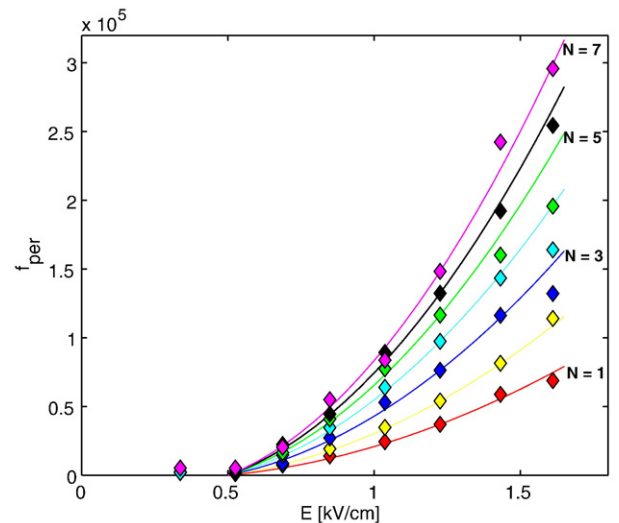

Fig. 7. The fraction of long-lived pores f_{per} after the N-th pulse obtained from measured conductivity changes (see Fig. 3) using Eq. (8) (symbols) compared to the predictions of the model according to Eq. (12) (lines).
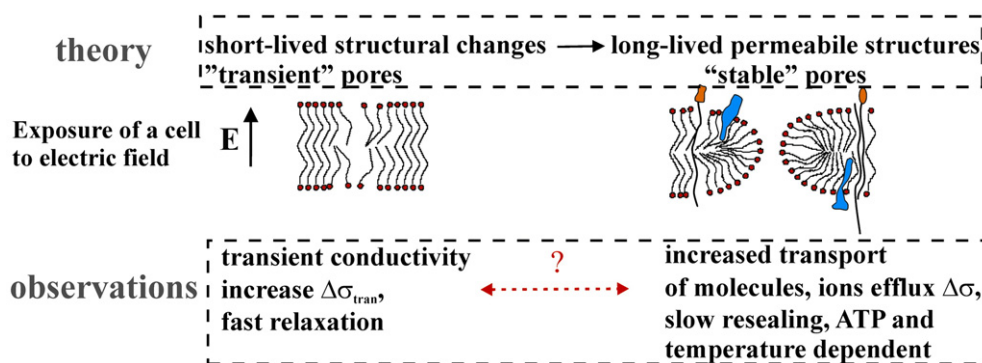
Fig. 8. Schematic representation of the relation between experimentally measured quantities (observables) and the theoretical interpretation.

percentage of permeabilized cells gradually increase with the number of pulses.

The similar transient changes can be explained with fast relaxation of transient conductivity changes obtained with combination of HV and LV pulses as well as with changing the repetition frequency, which was obtained to be around few milliseconds. Since relaxation of short–lived transient pores is fast, membrane conductivity decreases to an initial level after each pulse and when the next pulse is applied the cell membrane again behaves as an insulator. Therefore the value of the induced transmembrane voltage is the same for the second, third... eight pulse and since the induced transmembrane voltage governs the formation of short–lived pores is the fraction of these pores for each consecutive pulse the same. However, the nature of long–lived pores must be different then than that of the transient pores. Our results suggest that during each pulse a given fraction of transient pores is "stabilized" forming long–lived pores, however, since the pore fraction of these pores is much smaller compared to transient pores we can not detect them with conductivity measurements. Only few long–lived pores could suffice for a substantial uptake of molecules, eventhough-even though their contribution to the increase in conductivity is negligible. In contrast to transient pores, we can assume that when new pulse is applied again a certain number of long–lived pores are formed leading to increased permeability for several pulses as well as to linear increase in flow coefficient. This could explain the observed difference between increased permeability for several pulses compared to the constant fraction of transient pores for consecutive pulses.

The measured quantity which approximately correlates with the molecular uptake is conductivity change due to ion efflux $\Delta\sigma/\sigma_{max}$, and consequently also the flow coefficients k_N and the fraction of long-lived pores (f_{per}) since all approximately linearly increase with number of pulses. This is in agreement with molecular uptake (see

Table 2), which also increases with number of pulses [39–43]. The increase in f_{per} with N suggests that each individual pulse (independently on previous pulse) adds to formation/stabilization of new long-lived pores. The fraction of long-lived pores (f_{per}) depends also on the square of the electric field in the region which is exposed to above-critical voltage as shown in Fig. 8. This cannot be directly observed with molecular transport since in general the total transport is a complex time-dependent function, where among other parameters also resealing constant determines the amount of diffusion.

From the presented results it follows that ion diffusion can be used to determine the fraction of the long-lived pores (f_{per}) and long-lasting permeability (flow coefficient k_N) of the cell membrane. The transient conductivity changes, however, are similar for several pulses and thus represent only short-lived pores in the cell membrane that do not contribute to transport of molecules. This in agreement with other reports [23,24,26–28], which have shown that the transient conductivity changes (short-lived pores) are related to permeabilization (long-lived pores) only indirectly. Furthermore, f_p obtained from the transient changes is much larger than the fraction of long-lived pores f_{per} obtained from ion diffusion, clearly indicating that both quantities have to be analyzed separately.

Our results suggest that the fraction (number and/or size) of short-lived pores is at least an order of magnitude larger compared to long-lived pores, which is in agreement with other studies [23,24,26–28,33,36]. However, short life-time after the pulses indicates that these pores are not stable without the presence of the electric field and that only few of these pores remain present after the pulse. Possible explanations of pore stabilization are coalescence of smaller pores into larger [20], stabilization due to membrane structures (proteins, cytoskeleton) [14,44–46] or formation of long-lived pores due to structural discontinuities at domain interfaces [47]. In Fig. 8 we present possible visualization of what might be the short- and long-lived structural changes in the membrane. Here we have to stress that several independent studies showed that orientation of lipid head groups is involved in formation of transient pores during electric pulses [28,48,49], while only a single study [50] directly observed lipid head groups reorganization of long–lived permeable structures after the pulses by NMR spectroscopy. Therefore, the representation of short–lived and long–lived pores presented in Fig. 8 should be considered only hypothetically.

To summarize our main observations: i) The state of transiently increased membrane conductivity indicates the existence of short-lived membrane structures which enable ion permeation. The model of aqueous pores formation of electroporation corresponds to conductive hydrophilic pores [14]. An alternative explanation of these permeable structures is that they there are structural mismatches in the lipid organization [47]. The membrane conductivity drops to the initial level in a range of a millisecond after the pulses. This could be explained only with the existence of many small pores transient during the electric pulses, which close very rapidly (milliseconds)

Table 2
Comparison of the measured transient conductivity changes $\Delta\sigma_{tran}/\sigma_0$ during N-th pulse, changes of the initial level of conductivity due to ion efflux $\Delta\sigma/\sigma_0$ (after N pulses) and percentage of permeabilized cells is shown

Number of pulses	$N=1$	$N=2$	$N=4$	$N=8$
$\Delta\sigma_{tran}/\sigma_0$	0.15	0.14	0.14	0.145
$\Delta\sigma/\sigma_0$	0.083	0.2	0.4	0.59[a]
k_N [s^{-1}] 8×100 μs	0.029	0.040	0.072	0.11[a]
f_p [×10^{-5}]	~3	~3	~3	~3
f_{per} [×10^{-6}]	~1.4	~1.9	~3.4	~5.4[a]
% permeabilization[b]	10%	–	–	90%
% permeabilization[c]	14%	–	33%	75%

We further calculated permeability coefficient k_N the fraction of transient short-lived pores (f_p) and fraction of long-lived pores (f_{per}). All parameters are evaluated at $E \sim 0.86$ kV/cm ($E_0 \sim 1$ kV/cm).

[a] After seventh pulse − $N=7$ (diffusion between seventh and eight pulse).
[b] According to reference [42].
[c] According to reference [41].

after the pulse. The number of these short-lived pores does not depend on the number of applied pulses but solely on the electric field strength and pulse duration. Therefore by measuring transient conductivity changes during the electric pulses we can detect permeabilization threshold but not the level of permeabilization. ii) The state of increased permeability can last for several minutes after pulse application. Therefore it is clear, that in contrast to transient pores with fast resealing in milliseconds some pores are stabilized enabling transport across the membrane in minutes after the pulses. The quantification of ion efflux shows that in contrast to transient short-lived pores these more stable pores are governed both by electric field strength as well as the number of pulses. The fraction of long-lived pores increases with higher electric field due to larger area of the cell membrane exposed to above-critical voltage and due to higher energy which is available for pores formation. Moreover, each consecutive pulse increases the probability for the formation of the long-lived pores. iii) The resealing of the cell membrane is a biologically active process that strongly depends on the temperature and lasts from minutes to hours after pulse application and corresponds to resealing of long-lived pores, whereas fast relaxation of conductivity in milliseconds correspond to "fast resealing" of short-lived pores. This clearly shows that long-lived pores are thermodynamically stable also after pulse application whereas short-lived pores are not. All these observations lead to a conclusion that the nature of long-lived pores is different from that of short-lived pores, which are present only during or shortly after the pulses, and that molecular mechanisms which contribute to pore stabilization as well as the adequate theoretical description are yet to be determined.

Acknowledgements

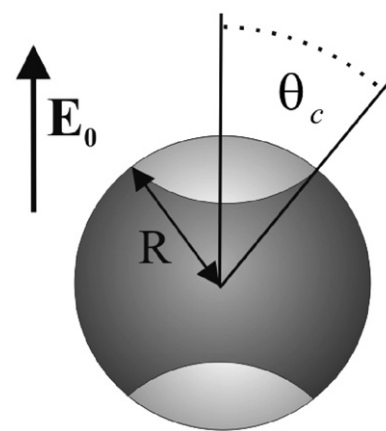## Appendix A. Diffusion through the permeabilized membrane

In the following we will derive the diffusion equation through the permeabilized membrane and determine the fraction of long-lived pores. In general the increase in membrane permeability can be described as the fraction of the permeable surface of the cell membrane which can be also defined as the fraction of all "transport" pores:

$$f_{per} = S_{por}/S_0. \tag{A.1}$$

where S_{por} represents the area of pores of one cell, S_0 total area of one cell and f_{per} represents the fraction of the pores which are large enough to contribute to increased diffusion for ions and molecules through the cell membrane. It was shown that diffusion of ions and molecules occurs only through the permeabilized area $S_c = S_0 (1 - E_c/E)$, i.e. through the area which is exposed to the above-critical voltage [27]. We can therefore derive a diffusion equation which describes the flux of a given molecule due to the concentration gradient through the permeable membrane:

$$\frac{dn_e(t)}{dt} = -\frac{c_e(t) - c_i(t)}{d} D f_{pc}(E, t_E, N)(1 - E_c/E) S_0, \tag{A.2}$$

where $f_{per} = f_{pc}(1 - E_c/E)$, and $f_{pc} = S_{por}/S_c$ represents the fraction of pores in the permeabilized region. The above equation is good approximation of ion and molecular diffusion, since diffusion is a relatively slow process which occurs mainly after the pulse application. Fig. A.1.

Fig. A.1. Schematic representation of a spherical cell exposed to the external electric field. The bright shaded part represents the area exposed to above-threshold transmembrane voltage $|U_m| > U_c$, i.e. the permeabilized region. Here we have to stress that this is only a schematic representation where we neglected the resting potential. The resting potential of the cell is superimposed to the induced potential, therefore the permeabilized caps are not of the same size. However, since the resting potential on one side increases while on the other decreases the permeabilized surface, the effect of the resting potential on the total surface area is negligible [51].

If we assume that volume fraction F and surface area of the pores S_{por} are approximately constant, we obtain that the solution of Eq. (A.2) is an exponential increase to maximum $c_e^{max} = F c_i^0$ (c_i^0 is the initial internal concentration):

$$c_e(t) = c_e^{max}\left[1 - \exp\left(-\frac{t}{\tau}\right)\right], \tag{A.3}$$

with a time constant τ and flow coefficient k being dependent on the fraction of long-lived pores f_{per}:

$$\tau = \frac{1}{f_{per}}\frac{3D}{dR(1 - F)}, \quad k = 1/\tau. \tag{A.4}$$

To determine the flow coefficients from conductivity measurements we have express the above quantities in terms of conductivity changes (detailed derivation is given in [38]). The flow coefficient after the N-th pulse can be determined from the measured conductivity between N-th pulse ($\Delta\sigma_N$) and at $N+1$-th pulse ($\Delta\sigma_{N+1}$) [3]:

$$k_N = \frac{1}{\Delta t_N} \ln\left[1 - \frac{\Delta\sigma_N}{\Delta\sigma_{max}}\middle/1 - \frac{\Delta\sigma_{N+1}}{\Delta\sigma_{max}}\right], \tag{A.5}$$

where Δt_N is the time difference between the N-th and $N+1$-th pulse (one second in case of 1 Hz repetition frequency), and $\Delta\sigma_{max}$ is the maximum value of the conductivity, i.e. the saturation point when the concentrations inside and outside the cell are equal. From the permeability coefficient k_N the fraction of pores can be estimated using Eq. (A.4):

$$f_{per} \approx k_N \frac{dR(1 - F)}{3D'}, \quad D' = D \exp\left(-0.43 w_0\right), \tag{A.6}$$

where we take into account the effective diffusion constant D' of potassium ions inside the pores [21].

References

[1] E. Neumann, K. Rosenheck, Permeability changes induced by electric impulses in vesicular membranes, J. Membr. Biol. 10 (1972) 279–290.
[2] U. Zimmermann, Electric field-mediated fusion and related electrical phenomena, Biochim. Biophys. Acta. 694 (1982) 227–277.
[3] E. Neumann, A.E. Sowers, C.A. Jordan, Electroporation and Electrofusion in Cell Biology, Plenum Press, New York, 1989.
[4] M. Okino, H. Mohri, Effects of a high-voltage electrical impulse and an anticancer drug on in vivo growing tumors, Jpn. J. Cancer Res. 78 (1987) 1319–1321.

[5] L.M. Mir, Therapeutic perspectives of in vivo cell electropermeabilization, Bioelectrochemistry 53 (2000) 1–10.
[6] G. Serša, S. Kranjc, M. Čemažar, Improvement of combined modality therapy with cisplatin and radiation using electroporation of tumors, Int. J. Radiat. Oncol. Biol. Phys. 46 (2000) 1037–1041.
[7] T.K. Wong, E. Neumann, Electric field mediated gene transfer, Biochem. Biophys. Res. Commun. 107 (1982) 584–587.
[8] E. Neumann, M. Schaefer-Ridder, Y. Wang, P.H. Hofschneider, Gene transfer into mouse lyoma cells by electroporation in high electric fields, EMBO J. 1 (1982) 841–845.
[9] M.J. Jaroszeski, R. Heller, R. Gilbert, Electrochemotherapy, Electrogenetherapy and Transdermal Drug Delivery: Electrically mediated Delivery of Molecules to Cells, Humana Press, New Jersey, 1999.
[10] F. Liu, S. Heston, L.M. Shollenberger, B. Sun, M. Mickle, M. Lovell, L. Huang, Mechanism of in vivo DNA transport into cells by electroporation: electrophoresis across the plasma membrane may not be involved, J. Gene Med. 8 (2006) 353–361.
[11] G.J. Prud'homme, Y. Glinka, A.S. Khan, R. Draghia-Akli, Electroporation-enhanced nonviral gene transfer for the prevention or treatment of immunological, endocrine and neoplastic diseases, Curr. Gene Ther. 6 (2006) 243–273.
[12] M. Marty, G. Serša, J.R. Garbay, J. Gehl, C.G. Collins, M. Snoj, V. Billard, P.F. Geertsen, J.O. Larkin, D. Miklavčič, D.I. Pavlović, S.M. Paulin-Košir, M. Čemažar, N. Morsli, D.M. Soden, Z. Rudolf, C. Robert, G.C. O'Sullivan, L.M. Mir, Electrochemotherapy — an easy, highly effective and safe treatment of cutaneous and subcutaneous metastases: results of ESOPE (European Standard Operating Procedures of Electrochemotherapy) study, Eur. J. Cancer Suppl. 4 (2006) 3–13.
[13] T.Y. Tsong, Electroporation of cell membranes, Biophys. J. 60 (1991) 297–306.
[14] J.C. Weaver, Y.A. Chizmadzhev, Theory of electroporation: a review, Bioelectrochem. Bioenerg. 41 (1996) 135–160.
[15] J. Teissie, M.P. Rols, An experimental evaluation of the critical potential difference inducing cell membrane electropermeabilization, Biophys. J. 65 (1993) 409–413.
[16] J. Teissie, M. Golzio, M.P. Rols, Mechanisms of cell membrane electropermeabilization: a minireview of our present (lack of ?) knowledge, Biochim. Biophys. Acta 1724 (2005) 270–280.
[17] D.P. Tieleman, H. Leontiadou, A.E. Mark, S.J. Marrink, Simulation of pore formation in lipid bilayers by mechanical stress and electric fields, J. Am. Chem. Soc. 125 (2003) 6282–6383.
[18] K.H. Schoenbach, B. Hargrave, R.P. Joshi, J.F. Kolb, R. Nuccitelli, C. Osgood, A. Pakhomov, M. Stacey, R.J. Swanson, J.A. White, S. Xiao, J. Zhang, S.J. Beebe, P.F. Blackmore, E.S. Buescher, Bioelectric effects of intense nanosecond pulses, IEEE Trans. Dielec. Elec. Insul. 14 (2007) 1088–1109.
[19] L.V. Chernomordik, S.I. Sukarev, S.V. Popov, V.F. Pastushenko, A.V. Sokirko, I.G. Abidor, Y.A. Chizmadzev, The electrical breakdown of cell and lipid membranes: the similarity of phenomenologies, Biochim. Biophys. Acta. 902 (1987) 360–373.
[20] I.P. Sugar, E. Neumann, Stochastic model for electric field-induced membrane pores electroporation, Biophys. Chem. 19 (1984) 211–225.
[21] R.W. Glaser, S.L. Leikin, L.V. Chernomordik, V.F. Pastushenko, A.V. Sokirko, Reversible electrical breakdown of lipid bilayers: formation and evolution of pores, Biochim. Biophys. Acta 940 (1988) 275–287.
[22] S.A. Freeman, M.A. Wang, J.C. Weaver, Theory of electroporation for a planar bilayer membrane: predictions of the fractional aqueous area, change in capacitance and pore–pore separation, Biophys. J. 67 (1994) 42–56.
[23] K. Kinosita, T.Y. Tsong, Formation and resealing of pores of controlled sizes in human erythrocyte membrane, Nature 268 (1977) 438–441.
[24] K. Kinosita, T.Y. Tsong, Voltage-induced conductance in human erythrocyte, Biochim. Biophys. Acta 554 (1979) 479–497.
[25] I.G. Abidor, A.I. Barbul, D.V. Zhelev, P. Doinov, I.N. Bandarina, E.M. Osipova, S.I. Sukharev, Electrical properties of cell pellets and cell fusion in a centrifuge, Biochim. Biophys. Acta, 1152 (1993) 207–218.
[26] M. Pavlin, M. Kandušer, M. Reberšek, G. Pucihar, F.X. Hart, R. Magjarević, D. Miklavčič, Effect of cell electroporation on the conductivity of a cell suspension, Biophys. J. 88 (2005) 4378–4390.
[27] K. Schwister, B. Deuticke, Formation and properties of aqueous leaks induced in human erythrocytes by electrical breakdown, Biochim. Biophys. Acta 816 (1985) 332–348.
[28] M. Schmeer, T. Seipp, U. Pliquett, S. Kakorin, E. Neumann, Mechanism for the conductivity changes caused by membrane electroporation of CHO cell-pellets, Phys. Chem. Chem. Phys. 6 (2004) 5564–5574.
[29] R.V. Davalos, B. Rubinsky, D.M. Otten, A feasibility study for electrical impedance tomography as a means to monitor tissue electroporation for molecular medicine, IEEE Trans. Biomed. Eng. 49 (2002) 400–403.
[30] D. Cukjati, D. Batiuskaite, F. André, D. Miklavčič, L.M. Mir, Real time electroporation control for accurate and safe in vivo non-viral gene therapy, Bioelectrochemistry 70 (2007) 501–507.
[31] R. Susil, D. Šemrov, D. Miklavčič, Electric field-induced transmembrane potential depends on cell density and organization, Electro. Magnetobiol. 17 (1998) 391–399.
[32] M. Pavlin, N. Pavšelj, D. Miklavčič, Dependence of induced transmembrane potential on cell density, arrangement and cell position inside a cell system, IEEE Tran. Biomed. Eng. 49 (2002) 605–612.
[33] M. Hibino, M. Itoh, K. Kinosita Jr., Time courses of cell electroporation as revealed by submicrosecond imaging of transmembrane potential, Biophys. J. 64 (1993) 1789–1800.
[34] M. Pavlin, D. Miklavčič, Effective conductivity of a suspension of permeabilized cells: a theoretical analysis, Biophys. J. 85 (2003) 719–729.
[35] K.A. DeBruin, W. Krassowska, Modeling electroporation in a single cell. I. Effects of field strength and rest potential, Biophys. J. 77 (1999) 1213–1223.
[36] M. Hibino, M. Shigemori, H. Itoh, K. Nagayama, K. Kinosita Jr., Membrane conductance of an electroporated cell analyzed by submicrosecond imaging of transmembrane potential, Biophys. J. 59 (1991) 209–220.
[37] E. Neumann, K. Toensing, S. Kakorin, P. Budde, J. Frey, Mechanism of electroporative dye uptake by mouse B cells, Biophys. J. 74 (1998) 98–108.
[38] M. Pavlin, V. Leben, D. Miklavčič, Electroporation in dense cell suspension — theoretical and experimental analysis of ion diffusion and cell permeabilization, Biochim. Biophys. Acta 1770 (2007) 12–23.
[39] M.P. Rols, J. Teissie, Electropermeabilization of mammalian cells: quantitative analysis of the phenomenon, Biophys. J. 58 (1990) 1089–1098.
[40] P.J. Canatella, J.F. Karr, J.A. Petros, M.R. Prausnitz, Quantitative study of electroporation-mediated molecular uptake and cell viability, Biophys. J. 80 (2001) 755–764.
[41] T. Kotnik, A. Maček-Lebar, D. Miklavčič, L.M. Mir, Evaluation of cell membrane electropermeabilization by means of a nonpermeant cytotoxic agent, BioTechniques 28 (2000) 921–926.
[42] A. Maček-Lebar, D. Miklavčič, Cell electropermeabilization to small molecules in vitro: control by pulse parameters, Radiol. Oncol. 35 (2001) 193–202.
[43] A. Maček-Lebar, G. Serša, S. Kranjc, A. Grošelj, D. Miklavčič, Optimisation of pulse parameters in vitro for in vivo electrochemotherapy, Anticanc. Res. 22 (2002) 1731–1736.
[44] M.P. Rols, J. Teissie, Experimental evidence for the involvement of the cytoskeleton in mammalian cell electropermeabilization, Biophys. J. 1111 (1992) 45–50.
[45] J. Teissie, M.P. Rols, Manipulation of cell cytoskeleton affects the lifetime of cell-membrane electropermeabilization, Ann. N.Y. Acad. Sci. 720 (1994) 98–110.
[46] M. Fošnarič, V. Kralj-Iglič, K. Bohinc, A. Iglič, S. May, Stabilization of pores in lipid bilayers by anisotropic inclusions, J. Phys. Chem. B 107 (2003) 12519–12526.
[47] J. Teissie, C. Ramos, Correlation between electric field pulse induced long-lived permeabilization and fusogenicity in cell membranes, Biophys. J. 74 (1998) 1889–1898.
[48] M. Kotulska, K. Kubica, S. Koronkiewicz, S. Kalinowski, Modeling the induction of lipid membrane electropermeabilization, Bioelectrochemistry 70 (2007) 64–70.
[49] A. Le Saux, J. Ruysschaert, E. Goormaghtigh, Membrane molecule reorientation in an electric field recorded by attenuated total reflection Fourier-transform infrared spectroscopy, Biophys. J. 80 (2001) 324–330.
[50] A. Lopez, M.P. Rols, J. Teissie, 31P-NMR analysis of membrane phospholipid organization in viable, reversibly electropermeabilized CHO cells, Biochemistry 27 (1988) 1222–1228.
[51] B. Valič, M. Pavlin, D. Miklavčič, The effect of resting transmembrane voltage on cell electropermeabilization: a numerical analysis, Bioelectrochemistry 63 (2004) 311–315.